Electron Dynamics of Silicon Surface States: Second-Harmonic Hole Burning on Si(111)-(7 × 7)

John A. McGuire,[1] Markus B. Raschke,[2] and Y. Ron Shen[1]

[1]*Department of Physics, University of California at Berkeley, Berkeley, California 94720, USA, and Materials Sciences Division, Lawrence Berkeley National Laboratory, Berkeley, California 94720, USA*

[2]*Max-Born-Institut für Nichtlineare Optik und Kurzzeitspektroskopie, D-12489 Berlin, Germany*

(Received 8 June 2005; published 28 February 2006)

We report the first all-optical study of homogeneous linewidths of surface excitations by the spectral-hole-burning technique with surface-specific second-harmonic generation as a probe. Measurement of transient spectral holes induced by a 100 fs pump pulse in excitations of the surface dangling-bond states of Si(111)-(7 × 7) led to a pump-fluence-dependent homogeneous linewidth as broad as ~100 meV or a dephasing time as short as 15 fs. The hole-burning spectra also revealed a strong coupling between the localized dangling-bond states and the associated surface phonon mode at 570 cm^{-1}. Carrier-carrier scattering was responsible for the linear dependence of the dephasing rate on pump fluence, and the carrier screening effect appeared to be weak.

DOI: 10.1103/PhysRevLett.96.087401 PACS numbers: 78.68.+m, 73.20.−r, 73.25.+i, 78.47.+p

The electron dynamics in solids determine the time scale and efficiency of charge and heat transport, charge screening [1], and pathways for excited carrier relaxation [2]. At *surfaces*, these processes can control photochemistry and influence the performance of electronic devices as their dimensions shrink. However, few studies have yet addressed the electron dynamics at surfaces [3–6].

Silicon's importance makes understanding its surface electron dynamics desirable. Si(111)-(7 × 7) has served as a model system for surface chemistry [7], surface phase transitions [8], and transport studies [9]. Understanding the evolution of nonequilibrium surface electronic excitations can clarify details of the coupling between electrons and between electrons and surface phonons [2,10].

In this study we apply surface second-harmonic generation (SHG) as a probe of transient spectral-hole burning, i.e., the surface-specific analogue of conventional bulk two-color pump-probe hole-burning spectroscopy. The widths of the observed spectral holes in the silicon dangling-bond (DB) states correspond to electronic dephasing times as short as 15 fs and are characterized by excitation-induced dephasing that indicates relatively weak screening of the carrier-carrier interactions. In addition, strong coupling between adatom electronic excitation and its optical-phonon frequency of 570 cm^{-1} is observed.

The surface second-harmonic (SH) response can be expressed in terms of a local, dipolar second-order source polarization $\boldsymbol{P}^{(2)}(2\omega) = \chi^{(2)}(2\omega;\omega)\mathbf{E}(\omega)\mathbf{E}(\omega)$ [11,12], where $\chi^{(2)}$ denotes the surface nonlinear susceptibility. In the surface-specific implementation of spectral-hole burning, we measure the SHG from a probe beam as a function of detuning relative to the pump beam at a fixed wavelength. The second harmonic of this probe pulse is then generated by a nonlinear susceptibility $\chi^{(2)}(2\omega_{\mathrm{pr}};\omega_{\mathrm{pr}};\omega_{\mathrm{pu}})$ that has been modified by the pump pulse [11,12].

Near the fundamental pump photon energy of 1.54 eV chosen in our experiments, the SHG response of Si(111)-(7 × 7) is characterized by two spectral features as shown in Fig. 1 [13,14]. The broad low-energy peak at ~1.2 eV is due to a one-photon resonant transition from the Si rest-atom band S_2 into the adatom U_1 DB surface states [13,14]. In contrast, the feature at a fundamental photon energy of ~1.7 eV arises from a two-photon resonance at 3.4 eV [13], which corresponds to the energy of the bulk E_1 transition and the energy between backbond bonding S_3 and antibonding U_2 states.

The DB contribution $\chi^{(2)}_{\mathrm{res},0}(2\omega_{\mathrm{pr}};\omega_{\mathrm{pr}})$ to the total surface nonlinear susceptibility $\chi^{(2)}$ at $\hbar\omega_{\mathrm{pr}} \sim 1.54$ eV can be expressed by a single resonant term due to a pair of surface states $|a\rangle$ and $|b\rangle$ (i.e., a resonance with $\omega_{\mathrm{pu}} \sim \omega_{\mathrm{pr}} \sim \omega_{ba}$).

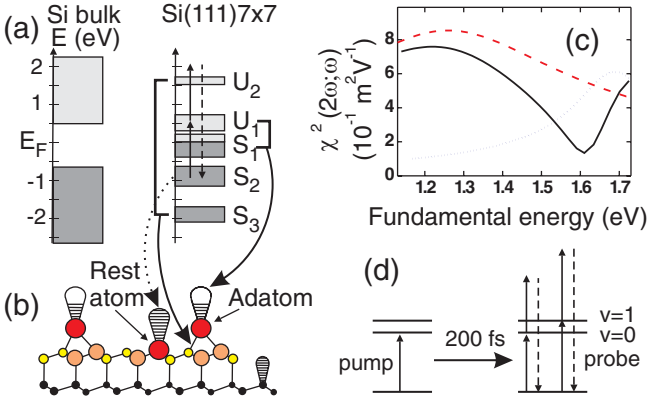

FIG. 1 (color online). (a) Surface-projected silicon bulk and surface band structure with adatom (S_1 and U_1) and rest-atom (S_2) dangling-bond and adatom-back-bond (S_3 and U_2) surface states [27]. (b) Ball-and-stick model of surface atoms indicating localized dangling-bond electrons. (c) SHG spectra for clean (solid curve) and hydrogen terminated (dotted curve), i.e., dangling-bond quenched, Si(111)-(7 × 7) (after [13,14]) and dangling-bond contribution (dashed curve) to the nonlinear susceptibility. (d) Three-level model for the S_2 to U_1 one-photon resonance discussed in the data analysis.

 © 2006 The American Physical Society

The large width of this DB resonance suggests that it is inhomogeneously broadened. The two-photon resonance at about 3.4 eV as well as any weak, completely nonresonant contributions are summarized by an effective nonresonant contribution $\chi^{(2)}_{\mathrm{NR}}(2\omega_{\mathrm{pr}};\omega_{\mathrm{pr}})$, which we consider as unaffected by the pump as discussed below. Then, in analogy to the case of bulk hole-burning spectroscopy, in the presence of a static inhomogeneous distribution $g(\omega_{ba})$ of resonant frequencies much broader than the homogeneous line width Γ_{ba}, $\chi^{(2)}$ can be expressed as

$$\chi^{(2)}(2\omega_{\mathrm{pr}};\omega_{\mathrm{pr}};\omega_{\mathrm{pu}}) = \chi^{(2)}_{\mathrm{NR}}(2\omega_{\mathrm{pr}};\omega_{\mathrm{pr}}) + \chi^{(2)}_{\mathrm{res},0}(2\omega_{\mathrm{pr}};\omega_{\mathrm{pr}}) \times \left\{1 - i\frac{I}{I_s}\frac{\Gamma_{ba}}{\Delta + i2\Gamma_{ba}}\right\}, \quad (1)$$

where $\Delta = \omega_{\mathrm{pr}} - \omega_{\mathrm{pu}}$, $\chi^{(2)}_{\mathrm{res},0}(2\omega_{\mathrm{pr}};\omega_{\mathrm{pr}})$ is the effective DB nonlinear susceptibility in the absence of the pump beam, and I and I_s are, respectively, the pump intensity and the saturation pump intensity [12]. The short time scales for incoherent population redistribution of a nonequilibrium electronic distribution in condensed systems require the hole-burning measurements to be performed transiently.

The experiments were performed in an ultrahigh vacuum (UHV) chamber with a base pressure of $<8 \times 10^{-11}$ mbar. Samples were cut from wafers of single-crystal, p-doped (1–2 Ω cm) Si and mounted on a liquid-nitrogen-cooled sample holder with the $[2\bar{1}\,\bar{1}]$ crystallographic axis oriented perpendicularly to the optical plane. The sample temperature was held at 80 K during the optical measurements. As verified by low-energy electron diffraction and Auger electron spectroscopy, clean and well ordered Si(111)-(7 × 7) surfaces were prepared following established procedures [13].

The pump pulses were taken from a Ti:sapphire oscillator/regenerative-amplifier system producing 1 mJ, 100 fs pulses at $\lambda = 805$ nm at a repetition rate of 1 kHz. Frequency doubling of the output of a β-BaB_2O_4-based continuum-seeded optical parametric amplifier [15] provided the probe beam. The pump and probe pulses each had a bandwidth of $\sim$200 cm^{-1} and a pulse length of about 100 fs ($\sim$2 times transform limit). To ensure uniform pumping, the probe beam was focused to a diameter $\sim$25% of that of the pump. As shown schematically in the inset of Fig. 2, the pump and probe beams were incident, respectively, at 47° and 43° with respect to the sample normal. The fluences at the sample surface were alternately set to 0.20, 0.40, 0.80, and 1.60 mJ/cm^2 for the pump and about 0.1 mJ/cm^2 for the probe beam, all well below the level at which two-photon absorption is expected to be significant [16]. From differential reflectivity measurements of Si(111)-(7 × 7) [17], this results in an estimated photogenerated surface carrier density ranging from approximately 0.25 to 2×10^{13} cm^{-2}, equivalent to 0.2 to 1.2 electron per 7 × 7 unit cell. Transit-time differences of the two beams across the beam spot on the surface effectively reduced the temporal resolution to about 200 fs. With the input pump, probe, and SHG output being p, s, and s polarized, respectively, the anisotropic nonlinear susceptibility tensor element $\chi^{(2)}_{|||||}$ was probed [11,12].

The resulting two-color pump/SHG-probe scans shown in Fig. 2 display a rapid, pump-induced decrease of the probe SHG signal. The subsequent recovery of the probe SHG signal on a time scale of several hundred fs provides the time scale of the relaxation of the excited- and ground-state population difference. The recovery of both negative- and positive-detuning data can be fit with single exponentials within the first several ps with recovery times of 730 ± 160 fs and 490 ± 90 fs, respectively.

The probe SHG is the result of an interference between the resonant dangling-bond contribution $\chi^{(2)}_{\mathrm{res}}(2\omega_{\mathrm{pr}};\omega_{\mathrm{pr}})$ and the effective nonresonant contribution $\chi^{(2)}_{\mathrm{NR}}(2\omega_{\mathrm{pr}};\omega_{\mathrm{pr}})$ [see Eq. (1)]. In order to extract the spectral-hole data for the dangling-bond excitations only, the relative phases and magnitudes between $\chi^{(2)}_{\mathrm{res}}$ and $\chi^{(2)}_{\mathrm{NR}}$ have been determined [18]. Figure 3 shows the resulting spectral hole induced by the dangling-bond excitation observed at a probe delay of 200 fs. As is particularly evident from the low-pump-fluence data, the results are characterized by a comparably weak hole at zero detuning followed by a second, more pronounced hole several hundred wave numbers to higher energies. The data can be fit using a modified version of Eq. (1) that models the effect of the pump as a pair of spectral holes at probe-pump detunings of $\delta = 0$ and $\delta = 570 \pm 100$ cm^{-1}:

$$\chi^{(2)}(2\omega_{\mathrm{pr}};\omega_{\mathrm{pr}};\omega_{\mathrm{pu}}) = \chi^{(2)}_{\mathrm{NR}}(2\omega_{\mathrm{pr}};\omega_{\mathrm{pr}}) + \chi^{(2)}_{\mathrm{res},0}(2\omega_{\mathrm{pr}};\omega_{\mathrm{pr}}) \times \{1 - i2\pi A_{\mathrm{F}}/(\Delta + i4\pi\Gamma_{\mathrm{F}}) - i2\pi A'_{\mathrm{F}}/(\Delta - 2\pi\delta + i4\pi\Gamma'_{\mathrm{F}})\}. \quad (2)$$

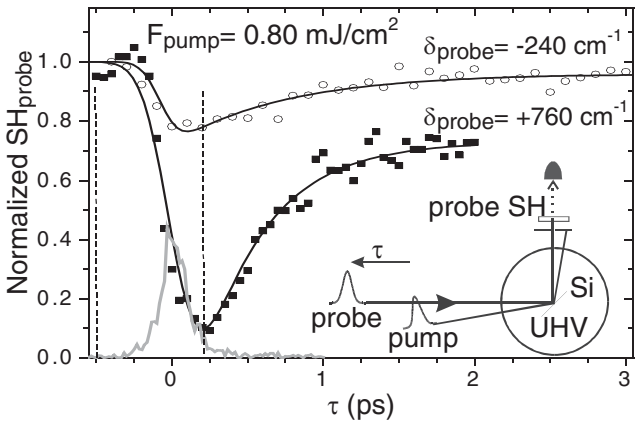

FIG. 2. Pump-SH$_{\mathrm{probe}}$ scans for probe-pump detunings $\hbar\omega_{\mathrm{pr}} - \hbar\omega_{\mathrm{pu}}$ of -29 meV (open circles) and -93 meV (solid squares) at a pump fluence of 0.80 mJ/cm^2. Data are normalized to the SHG signal at a probe delay of -500 fs. The solid lines serve as guides to the eye. The gray curve describes the sum-frequency cross correlation between pump and probe pulses. The vertical dashed lines indicate the times at which we measure the probe SHG to derive the spectral holes shown in Fig. 3. Inset: Schematic of the experimental layout.

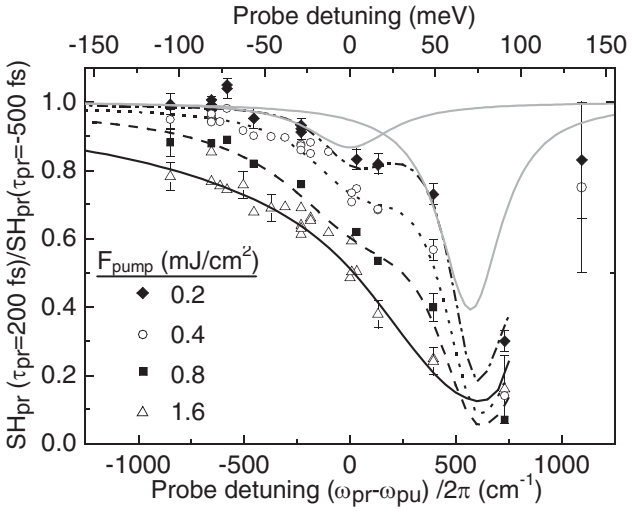

FIG. 3. Measured values of $\mathrm{SH_{pr}}(\tau_{\mathrm{pr}} = 200\ \mathrm{fs})/\mathrm{SH_{pr}}(\tau_{\mathrm{pr}} = -500\ \mathrm{fs})$ versus probe detuning at several pump fluences. The curves are fits to Eq. (2) using the parameters of Table I and the experimentally measured relative magnitudes and phases of $\chi^{(2)}_{\mathrm{res},0}$ and $\chi^{(2)}_{\mathrm{NR}}$. The gray curves show the individual spectral holes from Eq. (2) for the case of $\mathrm{F_{pump}} = 0.20\ \mathrm{mJ/cm^2}$.

The fit values of the parameters are given in Table I. The fit was restricted to $(\omega_{\mathrm{pr}} - \omega_{\mathrm{pu}})/2\pi < 750\ \mathrm{cm^{-1}}$, because at larger detunings the pump-probe trace was qualitatively different from those in Fig. 2, suggesting that other pumped excited states also contributed to the observed SHG at higher frequencies. In the data analysis, we treated the pulses as transform limited as the ~50 fs chirp is much below our temporal resolution.

As seen in Table I, the fitted values of Γ_{F} depend on pump fluence. The contribution of saturation broadening to Γ_{F} was estimated to be less than ~10% at the highest pump fluence. The width of the zero-detuned hole shows a linear dependence on pump fluence and translates into a homogeneous dephasing time of the order of tens of femtoseconds as indicated in Fig. 4 in which the rates have been corrected for contributions from the pump and probe linewidths. Extrapolation to zero pump fluence yields a dephasing time of ~100 fs.

The deep hole at a probe-pump detuning of 570 $\mathrm{cm^{-1}}$ implies strong coupling between the excited adatom electronic state and the 570 $\mathrm{cm^{-1}}$ surface optical phonon of Si(111)-(7 × 7) [20], which can be identified primarily with the out-of-plane motion of the adatom. Strong electron-phonon coupling at the adatoms has been implicated in the desorption of the adatoms of the Si(111)-(7 × 7) surface [21]. However, those measurements were performed at fluences 1 to 2 orders of magnitude higher than those used in our measurements, and the model did not identify the phonon modes involved. The observed coupling can be understood in terms of localization of both the electronic and the vibrational modes at the adatoms. These observations underly the three-level model shown schematically in Fig. 1(d). The initial state is associated with

TABLE I. Parameters for the two-Lorentzian holes in Eq. (2) used to fit the data for the pump-induced holes in Fig. 3 with $\delta = 570\ \mathrm{cm^{-1}}$.

Fluence [$\mathrm{mJ/cm^2}$]	A_{F} [$\mathrm{cm^{-1}}$]	Γ_{F} [$\mathrm{cm^{-1}}$]	A'_{F} [$\mathrm{cm^{-1}}$]	Γ'_{F} [$\mathrm{cm^{-1}}$]
1.60	$23(^{71}_{23})$	450(340)	364(160)	380(70)
0.80	80(10)	255(30)	100(10)	120(20)
0.40	34(5)	170(15)	90(10)	100(10)
0.20	16(3)	115(25)	60(5)	80(10)

rest atoms uncoupled to the adatom-derived phonon modes. The zero- and one-phonon transitions involve the excitation of the adatom DB with and without excitation of an optical phonon at 570 $\mathrm{cm^{-1}}$. However, in general and due to the fact that the spectral hole at positive detuning is deeper than the central hole, we cannot exclude that, e.g., Coulombic coupling of the DB excitation to the backbond resonance contributes to the observed spectral response.

As is evident from Fig. 4, a strong excitation-induced dephasing is observed. This suggests that carrier-carrier scattering is the dominant dephasing mechanism in the regime of higher pump energies. Defects and impurities may affect the equilibrium carrier density and hence the zero-fluence dephasing [22,23] but should not depend on the pump fluence. The apparent linear dependence on pump fluence parallels a similar observation for the rate of scattering into the unoccupied D_{down} states of the Si(111)-(2 × 1) surface observed in subpicosecond two-photon photoemission and attributed to electron-electron scattering [24]. Since two-photon excitation of carriers is negligible in comparison with linear excitation, the linear dependence on pump fluence indicates that electron screening of surface carrier interactions is weak [1]. This is consistent with the fact that electrons are more localized in the dangling bonds, or equivalently, the relevant surface bands are narrow. Recent β-NMR experiments of ^{8}Li adsorbed on the Si(111)-(7 × 7) surface provide evidence of the surface being near a Mott-Hubbard metal-insulator

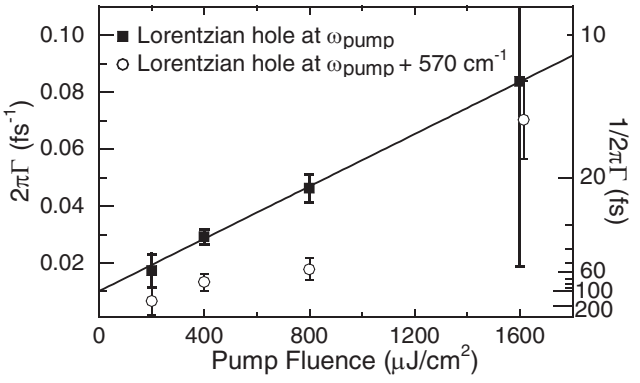

FIG. 4. Homogeneous dephasing rates deduced from the two-Lorentzian fit of the data versus pump fluence. Extrapolation to zero pump fluence yields an intrinsic homogeneous dephasing time of ~100 fs.

transition [25], which limits the ability of the electrons in the partially filled surface band at the Fermi energy to rapidly screen transient electronic excitations. Quantitative discussion on screening is unfortunately difficult because of a lack of detailed information on the surface states.

The ultrafast dephasing observed here can be compared with measurements of the homogeneous dephasing rates in the range of 20 to 30 fs determined for surface and image-potential states of Cu(111) [5,26] as well as previous experiments on Si(111)-(7 × 7). Although the surface carrier density in Si is much lower than in metals, strong screening in the latter greatly reduces the carrier-carrier scattering rate, leading to a dephasing rate comparable with that in Si. Our dephasing measurements on Si(111)-(7 × 7) are consistent with the preliminary result of the transient grating experiment of Voelkmann *et al.* [6]. Using 14 fs pulses and a pump fluence of 0.4 $\mathrm{mJ/cm^2}$, they obtained a grating decay time of ~5 fs, which corresponds to a dephasing time of ~20 fs in rough agreement with ours of 40 fs.

As suggested by our evidence for strong electron-phonon coupling, scattering with phonons should play an important role in the zero-fluence homogeneous dephasing. Time-resolved two-photon photoemission of carrier dynamics on Si(100)$c(4 \times 2)$ suggests that optical-phonon emission via deformation-potential scattering of excited DB electrons can occur on a time scale of ~300 fs [3]. Carrier-carrier scattering might also be a significant contribution to the zero-fluence homogeneous dephasing rate. Even in the limit of a single photoexcited electron-hole pair in the U_1 and S_2 bands, there are still electrons at or near the Fermi level in the adatom-derived S_1 band. These electrons could scatter coherently excited carriers.

In summary, we have presented the first measurement of homogeneous linewidths of surface electronic excitations by the hole-burning technique using surface-specific SHG as a probe. The results on excitations of the surface dangling-bond states of Si(111)-(7 × 7) revealed an excitation dephasing time linearly dependent on the pump fluence on the time scale of tens of femtoseconds. Carrier-carrier scattering was responsible for the observation. The hole-burning spectrum also showed the existence of strong coupling between the surface dangling-bond states and the surface phonon mode at 570 $\mathrm{cm^{-1}}$. For a more detailed understanding, however, more precise knowledge of the Si(111)-(7 × 7) surface electronic band structure is needed and many-body correlation effects should be included.

The authors acknowledge insightful discussions with K. Reimann and M. Wörner. This work was supported by the Alexander von Humboldt Foundation, Max-Planck-Society, and Director, Office of Science, Office of Basic Energy Sciences, Materials Sciences and Engineering Division, of the U.S. Department of Energy under Contract No. DE-AC03-76SF00098.

[1] W. Knox *et al.*, Phys. Rev. Lett. **61**, 1290 (1988); J.-Y. Bigot *et al.*, Phys. Rev. Lett. **67**, 636 (1991).
[2] Z. Wang *et al.*, Phys. Rev. Lett. **94**, 037403 (2005).
[3] M. Weinelt *et al.*, Phys. Rev. Lett. **92**, 126801 (2004).
[4] C. B. Harris *et al.*, Annu. Rev. Phys. Chem. **48**, 711 (1997).
[5] H. Petek *et al.*, Phys. Rev. Lett. **83**, 832 (1999); H. Petek and S. Ogawa, Prog. Surf. Sci. **56**, 239 (1997).
[6] C. Voelkmann *et al.*, Phys. Status Solidi A **175**, 169 (1999); Phys. Rev. Lett. **92**, 127405 (2004).
[7] H. N. Waltenburg and J. T. Yates, Chem. Rev. **95**, 1589 (1995); F. Tao and G. Xu, Acc. Chem. Res. **37**, 882 (2004).
[8] A. Mascaraque and E. Michel, J. Phys. Condens. Matter **14**, 6005 (2002).
[9] T. Tanikawa *et al.*, Phys. Rev. Lett. **93**, 016801 (2004).
[10] C. H. B. Cruz *et al.*, Chem. Phys. Lett. **132**, 341 (1986).
[11] T. Heinz, in *Nonlinear Surface Electromagnetic Phenomena*, edited by H.-E. Ponath and G. Stegeman (Elsevier, Amsterdam, 1991).
[12] Y. Shen, *The Principles of Nonlinear Optics* (John Wiley & Sons, New York, 1984).
[13] U. Höfer, Appl. Phys. A **63**, 533 (1996).
[14] T. Suzuki, Phys. Rev. B **61**, R5117 (2000).
[15] R. A. Kaindl *et al.*, J. Opt. Soc. Am. B **17**, 2086 (2000).
[16] T. Sjodin *et al.*, Phys. Rev. Lett. **81**, 5664 (1998).
[17] P. E. Wierenga *et al.*, Surf. Sci. **87**, 43 (1979).
[18] This was achieved by selective quenching of the DB contribution to $\chi^{(2)}_{\mathrm{res}}$ by H adsorption assuming that the magnitude and phase of $\chi^{(2)}_{\mathrm{NR}}$ are unaffected by H adsorption [13,19]). For 760 nm $\leq \lambda \leq$ 920 nm, the quantity $\chi^{(2)}_{\mathrm{res},0}/\chi^{(2)}_{\mathrm{NR}} = R\exp(i\phi_{\mathrm{NR}})$ could be well fit by the polynomial forms $\phi_{\mathrm{NR}} = 160° - 0.008\delta + 1.1\times10^{-5}\delta^2 - 2.1\times10^{-8}\delta^3 - 3.4\times10^{-11}\delta^4 - 1.2\times10^{-14}\delta^5$ and $R = 2.9\text{–}9\times10^{-4}\delta + 1.6\times10^{-6}\delta^2 - 1.4\times10^{-9}\delta^3 - 2.6\times10^{-12}\delta^4 - 8\times10^{-16}\delta^5$ for $\lambda_{\mathrm{pr}} < 864$ nm and $R = 4.1\text{–}6\times10^{-4}\delta$ for $\lambda_{\mathrm{pr}} > 864$ nm, where $\delta = \nu_{\mathrm{pr}} - 12\,500\ \mathrm{cm^{-1}}$.
[19] M. B. Yilmaz *et al.*, Phys. Rev. B **69**, 125413 (2004).
[20] W. Daum, H. Ibach, and J. E. Müller, Phys. Rev. Lett. **59**, 1593 (1987); J. Kim *et al.*, Phys. Rev. B **52**, 14 709 (1995).
[21] J. Kanasaki, K. Iwata, and K. Tanimura, Phys. Rev. Lett. **82**, 644 (1999); J. Kanasaki and K. Tanimura, Phys. Rev. B **66**, 125320 (2002).
[22] M. Weinelt *et al.*, Appl. Phys. B **68**, 377 (1999).
[23] M. Roth *et al.*, Phys. Rev. Lett. **88**, 096802 (2002).
[24] S. Tanaka and K. Tanimura, Surf. Sci. Lett. **529**, L251 (2003).
[25] R. Schillinger *et al.*, Phys. Rev. B **72**, 115314 (2005).
[26] E. Knoesel, A. Hotzel, and M. Wolf, J. Electron Spectrosc. Relat. Phenom. **88**, 577 (1998).
[27] R. J. Hamers, R. M. Tromp, and J. E. Demuth, Phys. Rev. Lett. **56**, 1972 (1986); P. Mårtensson *et al.*, Phys. Rev. B **36**, 5974 (1987); R. I. G. Uhrberg, T. Kaurila, and Y. C. Chao, Phys. Rev. B **58**, R1730 (1998); F. J. Himpsel and Th. Fauster, J. Vac. Sci. Technol. A **2**, 815 (1984).